Numerical Modeling of Wind Tunnel Walls for the Investigation of Oscillating Airfoils

Christoph Kaiser and Jens Nitzsche

Abstract The numerical modeling of airfoil oscillations in wind tunnels is investigated on the basis of frequency response functions of the flow field due to a forced motion input employing unsteady RANS simulations. The analyzed models reasonably predict the unsteady wind-tunnel wall effects, including the acoustic wind tunnel resonance. For high frequencies, however, the model shows significant spurious fluctuations related to non-physical reflections at the outflow boundary. Therefore, both increasing the distance to the computational boundaries and a nominally less-reflective boundary condition according to Hedstrom (1979, J. Comput. Phys. 30:222–237) are examined leading to slightly improved results.

1 Introduction

Unsteady aerodynamic simulation methods aiming at the prediction of dynamic loads and aeroelastic stability (flutter) need to be validated by unsteady wind tunnel experiments. For steady investigations in closed wind tunnels, adaptive walls provide a reasonable reduction of the wall effects by approximating a streamtube of an equivalent unconfined flow [14]. For unsteady cases like control surface oscillations [6] or gust excitations [9], however, the wall effects cannot be compensated by this approach. Thus, the numerical modeling of these experiments has to account especially for the wind-tunnel wall effects on the flow field [13].

The flow field around an oscillating airfoil in a wind tunnel can approximately be considered two-dimensional. Due to the wind tunnel's ceiling and floor, the dynamic lift experiences an increase in comparison to far-field conditions below the first acoustic resonance frequency of the wind tunnel. This resonance yields to a vanishing of the generated unsteady lift at the airfoil. Runyan et al. [8] provided an

C. Kaiser (✉) · J. Nitzsche
German Aerospace Center, Institute of Aeroelasticity, Göttingen, Germany
e-mail: christoph.kaiser@dlr.de

J. Nitzsche
e-mail: jens.nitzsche@dlr.de

A. Dillmann et al. (eds.), *New Results in Numerical and Experimental Fluid Mechanics X*, Notes on Numerical Fluid Mechanics and Multidisciplinary Design 132, DOI 10.1007/978-3-319-27279-5_40

experimental and theoretical confirmation of the resonance phenomenon and obtained for two-dimensional subsonic compressible flow the angular resonance frequencies of a plane wind tunnel:

$$\omega_n = (2n+1)\,\pi U_\infty \frac{\sqrt{1-Ma_\infty^2}}{Ma_\infty}\frac{1}{2b} \tag{1}$$

Equation 1 depends on the height $2b$ of the wind tunnel, the flow velocity U_∞ and Mach number Ma_∞ far away from the airfoil. The fundamental resonance frequency is obtained for $n = 1$.

For low Reynolds number flow, Ikeda et al. [3] numerically studied the tonal noise of a two-dimensional airfoil in a wind tunnel setup. By directly solving the compressible Navier-Stokes equations, they confirmed discrete tones associated with the resonance frequency proposed by Eq. 1.

In this paper, we investigate pseudo wind-tunnel walls, which are derived from an upper and lower streamline of a corresponding far-field solution. These pseudo wind-tunnel walls, on which slip conditions are applied, automatically account for the steady flow displacement and as such leave the steady solution unchanged. In the subsequent unsteady RANS simulations the frequency response of lift and surface pressure due to harmonic flap oscillations are computed and analyzed with emphasis on the post-resonance behavior.

2 Numerical Setup

In the following, the numerical setup for calculating the frequency response of a forced motion is described employing time-accurate RANS simulations.

2.1 Flow Solver

The time-accurate RANS computation is performed by the DLR TAU code with dual-time stepping according to Jameson [4] using a second-order backward differencing in time. The one-equation turbulence-model by Spalart and Allmaras [12] is used throughout this paper. The DLR TAU code [10] is a finite-volume, edge-based RANS solver for unstructured meshes using a node-centered approach.

2.2 Frequency Response Function

In order to identify the frequency response of the flow due to a harmonically oscillating airfoil, the forced motion simulation is conducted with a movement of very small

amplitude. This allows a linearized treatment around the steady flow state and thus, to identify the dynamic response over a range of frequencies by a single simulation through broadband excitation. Therefore, the motion affecting the airfoil is in the form of a short-time, small-amplitude pulse signal, see also [11].

The time-dependent motion according to the pulse function is realized via grid deformation at each time step, where the propagation of the prescribed surface deformation into the surrounding volume mesh is handled via radial basis function interpolation. The actual frequency response function is obtained by the ratio between the Fourier-transformed aerodynamic response and the Fourier-transformed input motion signal.

2.3 Grid Generation

The two-dimensional grid for the airfoil in a pseudo-wall wind tunnel is generated in three steps, see Fig. 1. At first, the steady far-field solution of the airfoil with the same inflow conditions as for the wind tunnel (flow velocity, Mach number, angle of attack) is computed on a unstructured far-field grid with a radius of 100 chord lengths and a structured boundary-layer mesh in the near-wall region. Secondly, from this far-field solution, two streamlines at the vertical distance b from the airfoil are extracted and define the upper and lower pseudo walls. Additionally, a perpendicular inflow and outflow boundary has to be introduced at a certain offset upstream and downstream of the airfoil. Finally, the grid around the airfoil is extracted from the original grid, cf. Fig. 2, and connected with a newly created unstructured mesh between the airfoil and each pseudo wall.

In order to reduce computational time, the cell sizes increase towards the inflow and outflow boundaries. The required grid resolution for the examined flow condition is found on the basis of a grid convergence study. The grids with large boundary offsets, however, are derived from the grid obtained for an offset of $10c$ by extending this grid with cells of constant size. This ensures the cells are not degenerated towards the new boundaries.

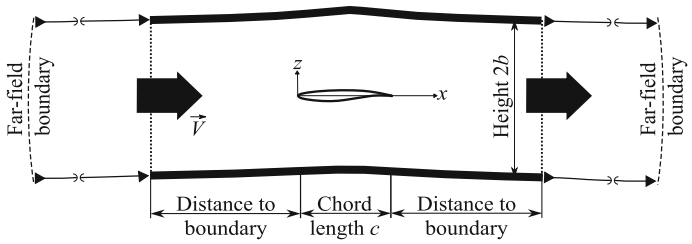

Fig. 1 Sketch of the wind tunnel geometry showing the airfoil, the streamline adapted walls, the inflow and outflow boundaries

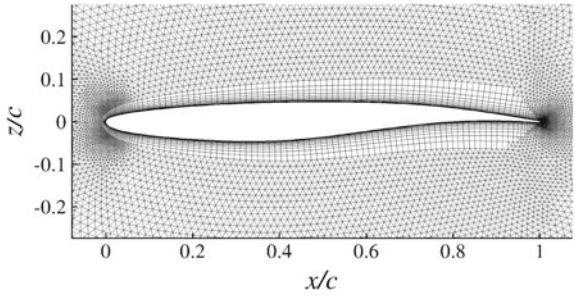

Fig. 2 Unstructured grid around the airfoil with a structured mesh of 30 layers in the vicinity of the boundary

2.4 Boundary Conditions

The boundaries of the generated grid comprise the upper and lower walls, the airfoil surface, the inflow and the outflow. The wind tunnel walls are modeled as Euler walls (i.e. slip condition) and thus, no additional boundary layer thickness has to be accounted for. The airfoil surface, in contrast, is defined physically correct as a no-slip wall.

At the inflow and outflow boundaries, far-field conditions are applied. In detail, the far-field constraints of the DLR TAU code are implemented according to Whitfield and Janus [15]. They are obtained by the analysis of the characteristics of the three-dimensional Euler equations, and are based on the assumption of one-dimensional, so-called straight flow, at the boundary. For the outflow, the approach of Whitfield and Janus results in a constant constraint for the pressure:

$$p = p_\infty \tag{2}$$

A constant pressure condition is known [7] to result in an increased reflective behavior for perturbations crossing the boundary. These reflected artifacts propagate upstream in subsonic flow and disturb, consequently, the pressure field around the airfoil. Hence, for this investigation, a less reflective outflow boundary condition is implemented into the DLR TAU code following the one-dimensional analysis of Hedstrom [2]. Hedstrom obtained a non-reflective boundary condition for one-dimensional hyperbolic systems, especially for the Euler equations. Accordingly, for the pressure, the following equation has to be fulfilled at the outflow:

$$\frac{\partial p}{\partial t} - \rho a \frac{\partial U}{\partial t} = 0 \tag{3}$$

In Eq. 3, a denotes the speed of sound, U the flow velocity and ρ the density at the boundary.

In summary, both formulations of the boundary conditions assume a one-dimensional flow and make use of the method of characteristics applied to the Euler equations in order to determine the flux over the boundaries. Consequently, they differ only in the equation related to the pressure.

3 Numerical Results and Discussion

The examined motions in this paper are flap oscillations in subsonic, compressible and viscous flow for the supercritical airfoil from [1] with a flap of 25 % chord length. Table 1 summarizes the applied simulation settings. Especially, the pulse's magnitude of the flap stroke has to be sufficiently small to guarantee linearity, cf. Sect. 2.2, which is ensured by a convergence analysis. Furthermore, the appropriate time step size for each examined grid is obtained through studying the convergence for the time discretization.

Figure 3 shows the comparison between the frequency response functions of the lift under far-field conditions and with pseudo wind-tunnel walls. The grid used for the unsteady far-field solution is a circular unstructured mesh with a radius of $100c$. The wind tunnel grid has an offset of $10c$ between the airfoil and the computational

Table 1 Parameter settings used for the forced motion simulations

Parameter	Symbol	Value
Mach number	Ma	0.5
Reynolds number	Re_c	2×10^6
Wind-tunnel height	$2b$	$3.33c$
Angle of attack	α	0°
Chord of flap	Λ	$0.25c$
Initial flap deflection	δ_0	0°
Pulse magnitude	δ_{max}	0.001°
Time-step size	$\Delta t \frac{U_\infty}{c}$	0.049
Inner iterations	-	600

The results in this paper are shown for $c = 1.0$

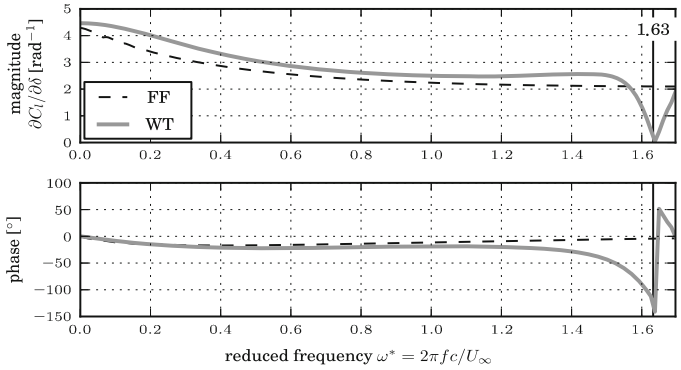

Fig. 3 Comparison between the frequency response of the lift under far-field conditions (FF) and with wind tunnel walls (WT) involving offsets of $10c$. The results illustrate the wind-tunnel wall effects of lift increase and resonance phenomenon for a flap oscillation with amplitude $\boldsymbol{\delta}$. The vertical line indicates the first resonance frequency according to Runyan et al. [8]

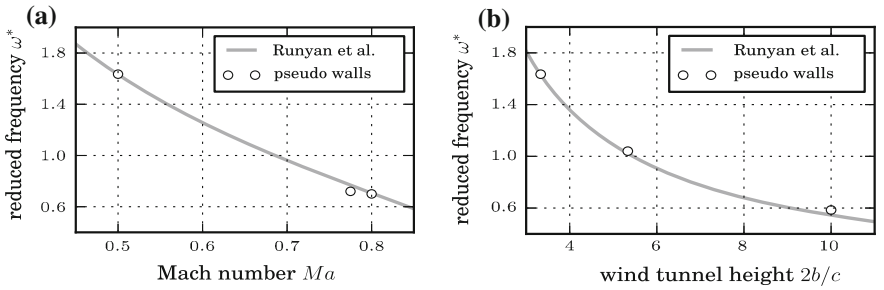

Fig. 4 Comparison of the fundamental frequencies according to Runyan et al. [8] and obtained by forced-motion simulations with pseudo wind-tunnel walls for: **a** different Mach numbers and $2b = 3.33c$, **b** different wind tunnel heights and $Ma = 0.5$

boundaries resulting in a length of $21c$. An increase of lift is found in the magnitude of the derivative $\frac{\partial C_l}{\partial \delta}$ followed by an abrupt decline. The drop occurs at the frequency predicted by Eq. 1 and thus, is attributed to wind-tunnel acoustic resonance. Indeed, the phase of the derivative shows a step of about 180° characteristically for a resonance condition. To this end, the comparison demonstrates the phenomena due to the wind-tunnel wall effects as described in Sect. 1.

Moreover, Fig. 4 shows the fundamental frequencies according to Eq. 1 in comparison to the frequencies assigned to the minimum of the lift's magnitude response in dependence of the Mach number and the height of the wind tunnnel.

The lift's frequency response beyond the resonance frequency is characterized by spurious fluctuations, see Fig. 5. To shed some light on these fluctuations, the frequency response of the pressure coefficient along the upper wall of the wind tunnel is analyzed. In Fig. 6a, the magnitude of the frequency response at each position is

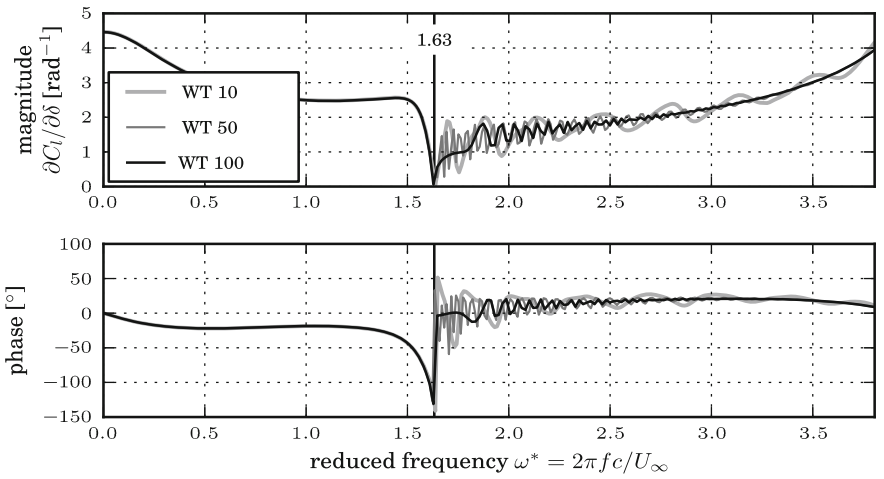

Fig. 5 Comparison of the frequency response functions of the lift for three wind tunnel grids with different offsets to the boundaries: $10c$ (WT10), $50c$ (WT50) and $100c$ (WT100)

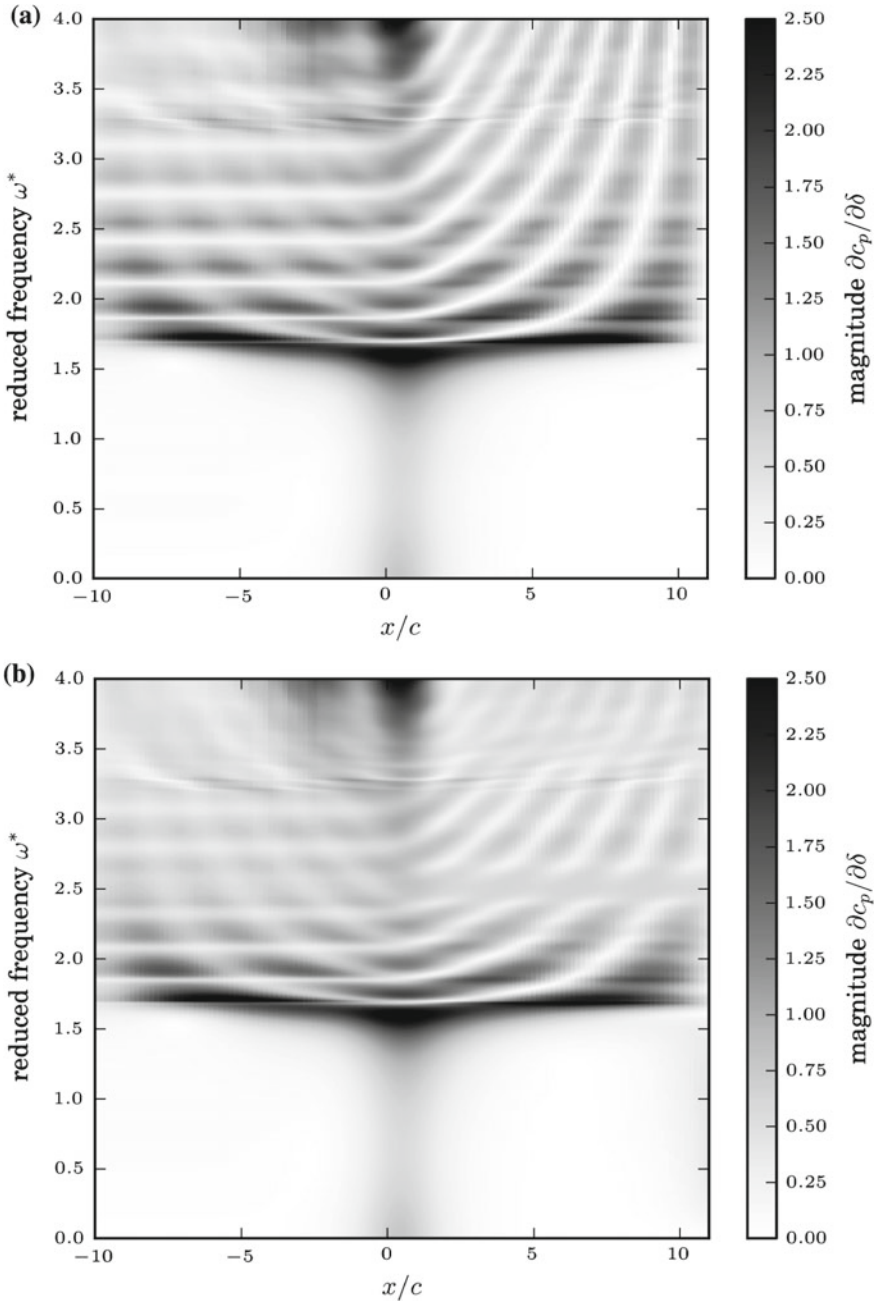

Fig. 6 Frequency response of the pressure coefficient along the ceiling of the wind tunnel with a boundary offset of $10c$: **a** outflow condition of Whitfield and Janus [15], **b** outflow condition of Hedstrom [2]. The shading indicates the magnitude of the frequency response

depicted in a contour plot with the reduced frequency on the ordinate. Below the resonance frequency, it shows an amplification only in the neighborhood of the airfoil. For higher frequencies an oscillatory pattern develops indicating standing waves in the tunnel. The wave numbers of the standing waves increase with the excitation frequency, while, at the same time, for all frequencies wave nodes can be observed at the outflow boundary. Consequently, these waves affect the pressure distribution around the airfoil resulting in the spurious fluctuations observed in the frequency response of the lift coefficient.

An increase of the inflow and outflow boundary offsets from $10c$ up to $100c$ results basically in the same spurious fluctuations but of smaller magnitude at higher frequency of occurence, see Fig. 5. Wave nodes recur on the outflow boundary and thus can be concluded to be an artifact of inadequate outflow boundary conditions.

Therefore, an alternative formulation of the outflow boundary condition, as described in Sect. 2.4, is investigated. Figure 6b displays the frequency response of the pressure coefficient along the ceiling wall for the nominally less-reflective boundary condition. Likewise, a wave pattern beyond the resonance frequency is observed. However, in comparison to Fig. 6a, the magnitude of the fluctuations is reduced overall and the wave nodes are less pronounced. Additionally, the wave nodes are no longer fixed at the outflow boundary which is, essentially, a result of the non-constant pressure condition.

4 Conclusion

The modeling of a two-dimensional wind tunnel was investigated by analyzing the frequency response functions due to unsteady airfoil oscillations. The expected wall effects were found in the results of the dynamic lift. However, the findings show a distinct influence of the computational boundaries, especially the outflow, for frequencies above the first acoustic resonance frequency of the wind tunnel. Standing waves emerge in the wind tunnel which are caused by reflections due to perturbations crossing the outflow boundary and lead to fluctuations in the frequency response. This is a known weakness of far-field boundary conditions with a constant pressure constraint.

Therefore, two different approaches for improving the boundaries were examined. Firstly, the boundaries have been moved away from the airfoil by extending the modeled length of the pseudo wind tunnel. This results in less pronounced fluctuations but at the cost of large grids accompanied by long computational times. It is unclear, whether simulations of very long wind tunnels together with a termination strategy, that does not allow reflective artifacts to reach the airfoil within the simulation time, could provide significant improvement. Secondly, the outflow boundary condition according to Hedstrom has been implemented into the DLR Tau code. This results in a damped wave pattern as observed for the frequency response of the pressure coefficient along the ceiling of the wind tunnel.

In conclusion, the investigated wall modeling predicts the first acoustic resonance frequency. For the accurate modeling at higher frequencies improved outflow

boundary conditions are necessary. The current implementation of the formulation of Hedstrom resulting from a one-dimensional analysis of the Euler equations is not capable of preventing reflections of more complex perturbations. Therefore, more sophisticated far-field boundary conditions like the Navier-Stokes characteristic boundary conditions [5] should be considered in further investigations.

References

1. Gardner, A.D., Richter, K., Rosemann, H.: Simulation of oscillating airfoils and moving flaps employing the DLR-TAU unsteady grid adaptation. In: Tropea, C., Jakirlic, S., Heinemann, H.-J., Henke, R., Hönlinger, H. (eds.) New Results in Numerical and Experimental Fluid Mechanics VI. 15th STAB/DGLR Symposium, Darmstadt, Germany, 2006. Notes on Numerical Fluid Mechanics and Multidisciplinary Design (NNFM), vol. 96. Springer, Heidelberg (2008)
2. Hedstrom, G.: Nonreflecting boundary conditions for nonlinear hyperbolic systems. J. Comput. Phys. **30**, 222–237 (1979)
3. Ikeda, T., Atobe, T., Konishi, Y., Nagai, H., Asai, K.: Numerical study of wind-tunnel acoustic resonance induced by two-dimensional airfoil flow at low Reynolds number. In: 29th Congress of the International Council of the Aeronautical Sciences, St. Petersburg, Russia, 7–12 September 2014
4. Jameson, A.: Time dependent calculations using multigrid, with applications to unsteady flows past airfoils and wings. In: 10th Computational Fluid Dynamics Conference, Honululu, 24–26 June 1991
5. Lodato, G., Domingo, P., Vervisch, L.: Three-Dimensional boundary conditions for direct and large-eddy simulation of compressible viscous flows. J. Comput. Phys. **227**, 5105–5143 (2008)
6. Nitzsche, J., Brouwers, K.J., Gardner, A.D., Mai, H., Dietz, G., Naudin, P., Leconte, P.: Investigation of unsteady control surface aerodynamics on a 2D supercritical airfoil model. 57. In: Deutscher Luft- und Raumfahrtkongress, Darmstadt, Germany, 23–25 September 2008
7. Rudy, D.H., Strikwerda, J.C.: A nonreflecting outflow boundary condition for subsonic Navier-Stokes calculations. J. Comput. Phys. **36**, 55–70 (1980)
8. Runyan, H.L., Woolston, D.S., Rainey, A.G.: Theoretical and Numerical investigation of the effect of tunnel walls on the forces on a oscillating airfoil in two-dimensional subsonic compressible flow. NACA Technical Note 3416 (1955)
9. Schmidt, H., Neumann, J., Mai, H.: Analysis of forced response in a wind tunnel based on Doublet-Lattice method. CEAS Aeronaut. J. **2**, 271–277 (2011)
10. Schwamborn, D., Gerhold, T., Heinrich, R.: The DLR TAU-Code: recent applications in research and industry. In: European Conference on Computational Fluid Dynamics, TU Delft, Netherlands (2006)
11. Seidel, D., Bennett, R., Whitlow, W. Jr: An exploratory study of finite difference grids for transonic unsteady aerodynamics. In: 21st Aerospace Sciences Meeting, Reno, Nevada, 10–13 January 1983
12. Spalart, P.R., Allmaras, S.R.: A one-equation turbulence model for aerodynamic flows. In: 30th Aerospace Sciences Meeting and Exhibit, January 1992
13. Voß, R.: Wall correction methods for dynamic tests. In: AGARDograph 336 Wind Tunnel Wall Corrections (1998)
14. Wedemeyer, E., Taylor, N.J., Holst, H.: Adaptive wall techniques. In: AGARDograph 336 Wind Tunnel Wall Corrections (1998)
15. Whitfield, D.L., Janus, J.M.: Three-Dimensional unsteady euler equations solution using flux vector splitting. In: AIAA 17th Fluid Dynamics, Plasma Dynamics, and Laser Conference, Snowmass, Colorado, 25–27 June 1984